A Quantitative Results-driven Approach to Analyzing Multisite Protein Phosphorylation

THE PHOSPHATE-DEPENDENT PHOSPHORYLATION PROFILE OF THE TRANSCRIPTION FACTOR PHO4*[S]

Francesca Zappacosta, Therese S. Collingwood, Michael J. Huddleston, and Roland S. Annan‡

Multisite protein phosphorylation appears to be quite common. Nevertheless our understanding of how multiple phosphorylation events regulate the function of a protein is limited in many cases. The ability to measure temporal changes in the site-specific phosphorylation profile of a protein in response to a given stimulus or cellular activity would provide an immediate indication of the functional significance of any phosphorylation site to a given process. Here we describe a mass spectrometry-based method to identify functionally relevant phosphorylation sites on a protein. It combines stable isotope labeling with a highly selective mass spectrometry analysis to detect and quantitate phosphorylation sites in response to a cellular signal. This approach requires no *a priori* knowledge of the phosphorylation state of the protein, does not require purification of phosphopeptides, and reliably detects substoichiometric levels of phosphorylation. Following a review of the quantitative results, only those phosphorylation sites that show a change in relative abundance are selected for identification and further study. We used this results-driven approach to study phosphorylation of the budding yeast transcription factor Pho4 in response to phosphate starvation. Phosphorylation of Pho4 on five cyclin-dependent kinase (Cdk) consensus sites has been shown to regulate the transcriptional activity of Pho4 in response to changes in environmental phosphate levels. Here we show that in phosphate-rich medium Pho4 is phosphorylated on at least 15 distinct sites including the five Cdk sites described previously. In excellent agreement with the known mechanism for regulation of Pho4 we found that phosphorylation at all five of the Cdk sites was repressed in phosphate-depleted medium. In addition to these five sites, we identified four novel phosphorylation sites that were also responsive to changes in phosphate availability. Selecting a limited number of Pho4 phosphorylation sites, we performed a more detailed kinetic analysis using an isotope-free strategy. We used LC-MS with selected reaction monitoring to greatly improve the accuracy, sensitivity, and dynamic range of the subsequent experiments. A detailed analysis of the cell-based phosphorylation at the selected Pho4 sites confirmed an apparent site preference for the Pho80-Pho85 cyclin-cyclin-dependent kinase complex. ***Molecular & Cellular Proteomics 5:2019–2030, 2006.***

Much of the activity in the cellular proteome is under the control of reversible protein phosphorylation. Phosphorylation-dependent signaling regulates differentiation of cells, triggers progression of the cell cycle, and controls metabolism, transcription, apoptosis, and cytoskeletal rearrangements. Signaling via reversible phosphorylation also plays a critical role in intracellular communication and the immune response. Phosphorylation can function as a positive or negative switch, activating or inactivating protein function (1). It can serve as a recognition element, targeting a substrate for ubiquitin-dependent proteolysis (2), or serve as a docking site to recruit other proteins into multiprotein complexes (3). Phosphorylation can trigger a change in the three-dimensional structure of a protein or initiate translocation of the protein to another compartment of the cell (4). Disruption of normal cellular phosphorylation events is responsible for a number of human diseases (5). Protein kinases, the enzymes responsible for phosphorylation, represent a very large gene family. In the human genome 518 kinases have been identified (6). Although this number is somewhat smaller than predicted prior to the completion of the human genome sequence, it still represents 1.7% of all human genes. Not surprising given the large number of protein kinases, as many as 30% of all the proteins in a cell are thought to be phosphorylated at any particular time (7). A single protein can be phosphorylated by several protein kinases on the same site or on different sites to varying stoichiometry. Each of these sites may be dephosphorylated by protein phosphatases at different times.

Knowledge of the specific amino acids phosphorylated on a protein is a critical component in assembling a complete understanding of a biological pathway. Although phosphosite mapping by several techniques including mass spectrometry is now fairly reliable, understanding which phosphorylation sites modulate protein function or are active in a given biological pathway is still a difficult problem. Adding to the complexity of this problem is the fact that phosphorylation-dependent function may not depend on activity at a single site

From the Proteomics and Biological Mass Spectrometry Laboratory, Department of Computational, Analytical and Structural Sciences, GlaxoSmithKline, King of Prussia, Pennsylvania 19406

Received, June 27, 2006

Published, MCP Papers in Press, July 6, 2006, DOI 10.1074/mcp.M600238-MCP200

but rather be dependent upon serial activation of several sites (8) and that multiple phosphorylation sites on a given protein may control multiple functions (9). Multisite phosphorylation of individual proteins appears to be quite common and may be more the rule than the exception (7). To unravel phosphorylation-dependent structure-function relationships, a quantitative analysis of site-specific protein phosphorylation would be useful. Changes in the stoichiometry at specific phosphorylation sites in response to stimulation of the cell or a change in its environment speaks to the physiological relevance of that site. Logically then, one would quantitate changes in phosphorylation stoichiometry in response to a cellular perturbation and then concentrate further study only on those sites that change in response.

Stable isotope labeling of peptides has been shown to be an effective method for deriving quantitative information on protein abundance (10–15). More recently, the incorporation of stable isotope labels into peptides either via chemical methods or metabolic labeling in cell culture has been shown to provide direct quantitative data on site-specific protein phosphorylation either on individual proteins (13, 16, 17) or from complex mixtures (18–20). Unlike the determination of protein abundance, however, where any peptide derived from the protein can be used for quantitation, site-specific phosphorylation analysis requires that specific peptides be detected and analyzed. In cases where the phosphorylation sites are known, the mass spectrometer can be used with great sensitivity to selectively target individual epitopes for quantitation (17). Of greater interest, however, is the application of a quantitative approach to understanding phosphorylation-dependent function in samples where the phosphorylation profile is not known. The most commonly adopted strategy to accomplish this has been to first identify as many phosphopeptides as possible in an isotopically labeled sample and then return to the data to derive quantitative information on the identified epitopes (16, 18–20). The major limitation of this approach is that a phosphopeptide must be identified before it can be quantitated. Even for simple mixtures, some form of enrichment (21, 22) is usually required to allow the efficient identification of phosphopeptides in the presence of what usually amounts to an overwhelming amount of non-phosphorylated peptides.

To improve the efficiency for finding functionally relevant phosphorylation sites in proteins we have applied a results-driven strategy (15, 23, 24) where, using stable isotopes, we quantitate all phosphopeptides in a sample first and then target for identification and further study only those peptides whose phosphorylation levels show a change. Isotope-labeled phosphopeptides are selectively detected in simple mixtures, such as SDS-PAGE-purified proteins, by mass spectrometry using a precursor ion scan for the phosphate marker ion PO_3^- (25, 26). This approach requires no *a priori* knowledge of the phosphorylation state of the protein, does not require purification of phosphopeptides, reliably detects substoichiometric levels of phosphorylation, and works equally well for serine, threonine, and tyrosine phosphorylation. We tested the ability of this approach to identify functionally relevant phosphorylation sites by quantifying the phosphorylation profile of the yeast transcription factor Pho4. The activity of Pho4 is regulated by phosphorylation in response to changes in the phosphate concentration of its environment (8, 27–29).

EXPERIMENTAL PROCEDURES

Reagents—*O*-Methylisourea sulfate salt was purchased from ICN Biomedicals, Inc. d_{10}-Propionic anhydride was synthesized by Cambridge Isotope Laboratories, Inc. with 98% atom purity. d_0-Propionic anhydride was purchased from Aldrich.

Protein Purification—A mammalian protein kinase that is activated by autophosphorylation on tyrosine was expressed as a GST fusion protein in Sf9 cells. After affinity enrichment on glutathione-Sepharose resin, the protein was autoactivated using Mg^{2+}-ATP. Protein samples were further purified by SDS-PAGE, and bands were stained with colloidal Coomassie Blue. Gel-purified samples were reduced, alkylated, and digested with trypsin as described previously (30). To study differential phosphorylation, activated and non-activated protein samples were combined in different ratios to yield protein samples representing 7, 37, and 70% phosphorylation stoichiometry at the activation site. Phosphorylation stoichiometry was determined by LC-MS using the peak intensity of the phosphorylated peptide and the non-phosphorylated counterpart.

The yeast transcription factor Pho4 was purified as either a GST or HA[1] fusion protein. The GST-Pho4 fusion protein was from the wild type yeast strain *572[pGST-PHO4]*. Yeast was grown to saturation at 30 °C in SC medium lacking uracil (SC−ura) (phosphate-rich medium). Saturated cultures were diluted to an A_{600} of 0.01 into either phosphate-rich or phosphate-depleted SC−ura medium (41). Expression of GST-Pho4 was induced upon addition of 0.5 mM $CuSO_4$ for 2 h at 30 °C. Pelleted cells were resuspended in extraction buffer (50 mM Tris-HCl, pH 7.5, 1 mM EDTA, 4 mM $MgCl_2$, 5 mM DTT, 10% glycerol, 1 M NaCl) and lysed with a bead beater. Supernatant was purified on glutathione-Sepharose resin.

The HA-Pho4 yeast strain (source, GenBank™ accession number YFR034C) was ordered from Openbiosystems. The yeast was grown and lysed according to the manufacturer's recommendation with modifications. Briefly saturated cultures were grown first in SC−ura containing dextrose and then transferred to raffinose. The culture was diluted and grown again to A_{600} of 0.8 before inducing the production of HA-Pho4 with 2% galactose. Cultures were grown in either phosphate-rich or phosphate-depleted medium as indicated. Yeast lysates were added to HA-agarose-conjugated beads, incubated at 4 °C overnight, and washed with 3 ml of lysis buffer.

Fusion proteins were further purified by SDS-PAGE and stained with colloidal Coomassie Blue. Gel bands were reduced, alkylated, and digested with trypsin as above. Pho4 from phosphate-rich medium was labeled with d_5, and Pho4 from the phosphate-depleted medium was labeled with d_0 as described below. For time course experiments, saturated cultures were transferred into phosphate-depleted SC medium to a final A_{600} of 0.1. After inducing Pho4 expression as described, cycloheximide was added to the cultures (final concentration of 100 μg/ml) and incubated for 30 min at 30 °C. One-fifth of the total culture volume was pelleted as a phosphate-free

[1] The abbreviations used are: HA, hemagglutinin; SC, synthetic complete; Cdk, cyclin-dependent kinase; SRM, selected reaction monitoring; NIT, N-terminal isotope tag.

control and flash frozen. Phosphate (20 mM KH_2PO_4) was added to the remaining culture, and equal aliquots were harvested at 20, 40, and 80 min; pelleted; and flash frozen. Pho4 was purified from each time point as described above.

Isotope Labeling—N-terminal isotope tags (NIT) were added to each peptide as described previously (15). Briefly an equal volume of 2 M *O*-methylisourea in 100 mM $NaHCO_3$, pH 11.0, was added to the peptide mixtures in 100 mM NH_4HCO_3, pH 8.5, and the sample was incubated for 2 h at 37 °C. Acylation with either d_0-propionic or d_{10}-propionic anhydride was carried out by adding 0.5 μl of reagent/sample and incubating for 30 min at 37 °C. The d_0- and d_5-labeled samples were pooled, and the excess reagent was removed by desalting on a C_{18} MicroTrap cartridge (Michrom BioResources, Inc.). Peptides were eluted in 30 μl of 60% ACN in 0.1% TFA. The volume was reduced to 5 μl in a SpeedVac. To promote hydrolysis of propionyltyrosine residues, 5 μl of water and 1 μl of 10 M NH_4OH (pH 11.0) was added to the samples and incubated for 1 h at 37 °C. The samples were acidified by addition of an appropriate volume of 10% TFA and stored at −20 °C.

Quantitation Using Phosphopeptide Selective Precursor Ion Scanning—An aliquot of the d_0/d_5 isotope-labeled sample (typically 25%) was concentrated on a C_{18} ZipTip (Millipore) and eluted with 2:1 methanol/ammonium hydroxide (30%, v/v) and loaded into a nanospray needle for analysis. Precursor ion spectra for *m/z* 79 were recorded on a Sciex API 3000 triple quadrupole mass spectrometer equipped with a nanoelectrospray source and operated in the negative ion mode. Isotope ratios were calculated using peak top intensities from the precursor ion spectra. Ratios were normalized for differences in protein load using the average ratio for 10 non-phosphorylated peptides from the same sample as determined in a separate LC-MS or MALDI-MS experiment.

Peptide Sequencing—Phosphopeptides whose NIT-labeled pairs showed a ratio lower than 0.7 or greater than 1.3 were targeted for sequencing by LC-electrospray MS/MS either on an Agilent LC-MSD ion trap or on a Micromass Q-TOF instrument. Peptides were loaded on a trap cartridge and back-flushed at 300 nl/min to a 75-μm-inner diameter C_{18} Zorbax column (15 cm) or to a 75-μm-inner diameter PepMap C_{18} column (15 cm) using a gradient of acetonitrile/water containing 0.1% formic acid.

Quantitation Using Selected Reaction Monitoring—Twelve precursor-fragment ion transitions were monitored to quantitate the Pho4 phosphorylated peptides and their non-phosphorylated counterparts. Several of the peptides were monophosphorylated on more than one site, but because they separated chromatographically, we chose a transition common to each set and distinguished them by retention time. Individual precursor-fragment ion transitions and the optimal collision energies for each were chosen from the MS/MS spectra used to identify the peptides. Each transition was acquired for 100 ms with the total cycle time for all 10 being 1.0 s. The entire cycle was repeated continuously during the LC-MS analysis of each time point. Analyses were performed on a Sciex 4000 QTRAP triple quadrupole mass spectrometer coupled to a nanoliter flow HPLC instrument equipped with a 75-μm-inner diameter PepMap C_{18} column (15 cm). Quantitation of each isoform was done by the Applied Biosystems Analyst software using the extracted ion current for each transition.

RESULTS AND DISCUSSION

Multisite phosphorylation of proteins appears to be quite common. A quantitative view of how the phosphorylation profile of a protein changes in response to a given stimulus or cellular activity would permit facile identification of those phosphorylation sites that are functionally relevant in a given process. To compare the phosphorylation state of a protein under two different conditions we have combined an isotope labeling strategy that selectively tags the N terminus of each peptide in a sample (15, 31) with a highly selective mass spectrometry experiment (25, 26). By labeling the N terminus of each and every peptide, we can theoretically quantitate any and all potential phosphorylation sites within a protein. Proteins from control or resting cells are labeled with a d_0 tag, and proteins from stimulated cells are labeled with a d_5 tag. After combining the labeled samples, the mixture is analyzed for phosphorylation content using precursor ion scanning mass spectrometry (25, 26). A scheme outlining the experimental process is shown in Fig. 1*A*.

Under collision-induced dissociation conditions, in the negative ion mode, phosphopeptides fragment in the mass spectrometer to produce the highly diagnostic marker ion $[PO_3]^-$ (*m/z* 79). By performing a precursor ion scan for *m/z* 79, the mass spectrometer detects only those peptides that can fragment to produce $[PO_3]^-$. Low abundance, low stoichiometry phosphorylation sites can be selectively detected in the presence of an excess of non-phosphorylated peptides even in cases where the signal from the phosphopeptide is indistinguishable from background in the conventional MS scan. Therefore, it is not necessary to isolate or purify the phosphopeptides prior to the quantitative analysis. In fact, it is not even necessary that the phosphorylation sites be known. Phosphorylation sites that are shown to be functionally significant based on a change in the d_0/d_5 ratio can then be identified, whereas those whose d_0/d_5 ratios remain unchanged can be ignored.

The first step in the evaluation of the NIT labeling protocol for quantitating protein phosphorylation was to test whether phosphopeptides were stable under the basic labeling conditions used in the NIT chemistry. To do this we incubated tryptic digests from four phosphoproteins in the pH 11 NIT buffer and monitored the stoichiometry of 11 different phosphoserine or phosphothreonine peptides by LC-MS. In all cases, we found the stoichiometry unchanged (data not shown).

To validate the NIT-precursor ion scan strategy for quantifying site-specific protein phosphorylation, we analyzed changes in phosphorylation stoichiometry at a phosphotyrosine residue in the activation loop of a protein kinase. We combined activated and non-activated protein in different proportions to produce three samples with stoichiometry at the activation site of 7, 35, and 70%. After digestion with trypsin, each of the three samples was split and labeled with either a d_0 or a d_5 tag. Combining aliquots of the various d_0- or d_5-tagged proteins (with the light tag acting as the wild type or control), we produced four samples with differential protein phosphorylation in the theoretical ratios of 0.10, 0.20, 0.50, and 1.0 (for instance by combining one aliquot of the d_0-labeled 35% protein and one aliquot of the d_5-labeled 70% protein we produced a sample with differential phosphorylation in the ratio of 0.5). Each of the four unfractionated sam-

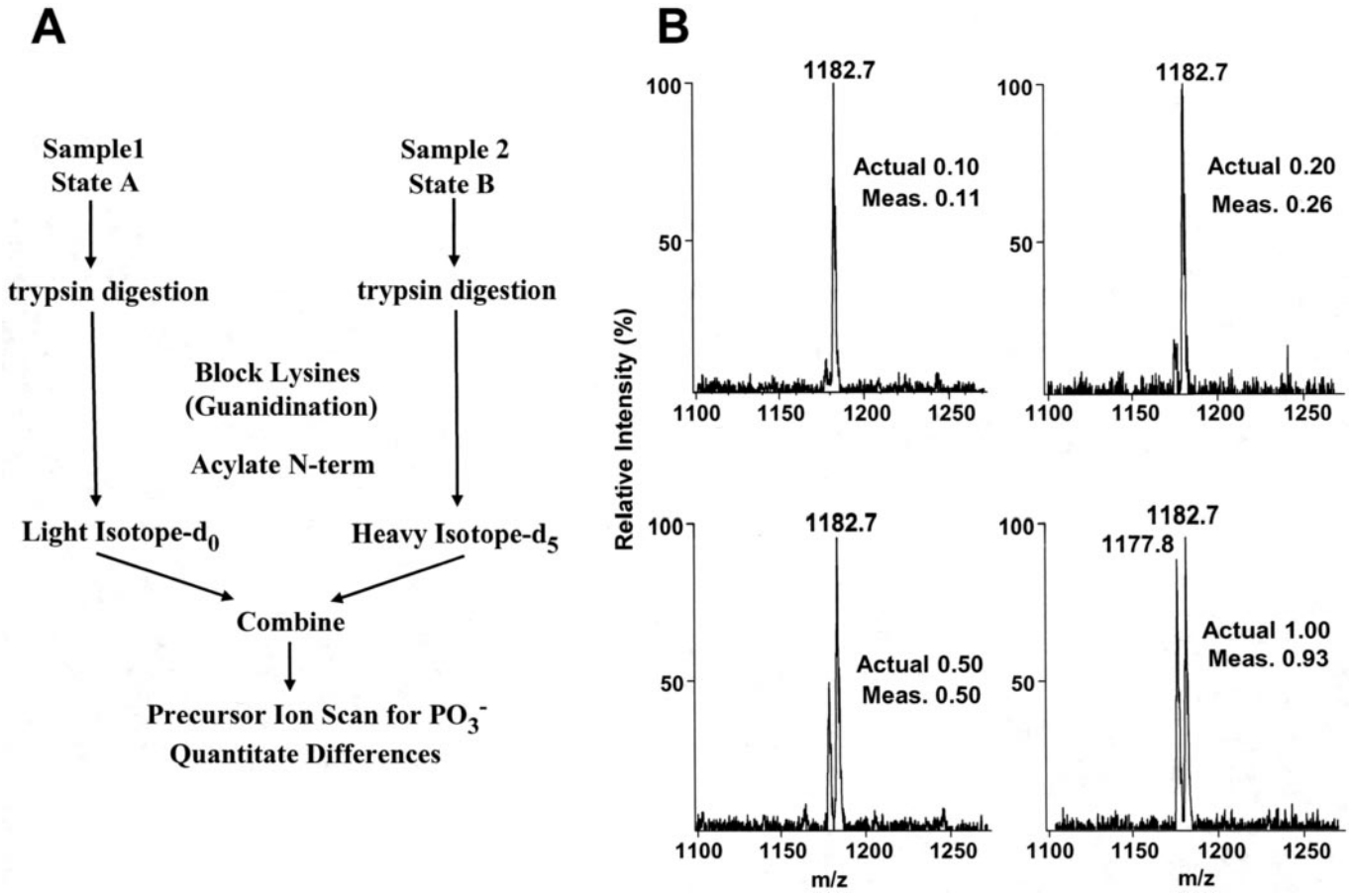

FIG. 1. **Quantitative analysis of protein phosphorylation using stable isotope labeling and precursor ion scanning.** *A*, schematic diagram of the process to quantitate changes in protein phosphorylation. *B*, validation of the NIT-precursor ion scan strategy for quantitating site-specific protein phosphorylation. Partial precursor ion mass spectra from four pairs of differentially phosphorylated proteins are shown. Tryptic digests of protein kinase samples phosphorylated to differing degrees were labeled with either a d_0 or d_5 tag, combined in known ratios, and analyzed by mass spectrometry without fractionation or enrichment for phosphopeptides. The observed ratio for each pair of the singly charged peptides compares well with the expected values. Correction factors for the observed ratios ranged from 0.99 to 1.06. The data shown are representative of replicate analyses using various d_0/d_5 ratios.

ples was analyzed for phosphorylation content using a precursor ion scan for *m/z* 79, and the relative difference in phosphorylation in each sample was determined using the d_0/d_5 ratio. The precursor ion scan spectrum for each of the four samples is shown in Fig. 1*B*. The peptide pair at *m/z* 1177 and 1182 corresponds to the singly charged d_0- and d_5-labeled peptide containing the tyrosine residue that is phosphorylated upon activation. To correct for differences in the amount of starting protein, a normalization factor was generated for each NIT-labeled sample by determining the d_0/d_5 ratio by LC-MS for 10 non-phosphorylated peptides from each sample. Normalization factors for the four samples ranged from 0.99 to 1.06. Although in this case such a contribution seems negligible, normalization of the phosphopeptide data is essential when studying *in vivo* derived samples where the exact protein starting amount cannot be accurately determined or where the overall abundance of the protein can be affected by a change in expression or degradation rates. After normalization the differential phosphorylation for the four samples was found to be 0.11, 0.26, 0.50, and 0.93 in good agreement with the predicted values (Fig. 1*B*). Again it is important to note that these measurements were made without purifying the phosphopeptides and that the analysis was done from the unfractionated tryptic digest of the protein.

Phosphorylation Analysis of Pho4—In budding yeast the transcription factor Pho4 regulates the expression of genes needed by the organism to respond to phosphate starvation (32). The transcriptional activity of Pho4 is regulated in response to the availability of phosphate by the cyclin-cyclin-dependent kinase (Cdk) complex Pho80-Pho85 (33). Under conditions of normal phosphate availability, Pho4 is phosphorylated on multiple sites and exported from the nucleus (27), preventing unnecessary expression of phosphate responsive genes. Pho4 contains six SerPro sites, S1 (Ser^{100}), S2 (Ser^{114}), S3 (Ser^{128}), S4 (Ser^{152}), S5 (Ser^{204}), and S6 (Ser^{223})

TABLE I
Phosphopeptides from Pho4 grown in phosphate-rich medium

Peak	MW_{det}[a]	Pho4[b]	Sequence[c]	Residue
1	3575.7	80–110 + P	AFELVEGMDMDWMMPSHAHH**pS**PATTATIKPR	Ser^{100} (S1)
2[d]	3476.4	111–143 + P	LLY**pS**PLIHTQSAVPVTISPNLVATATSTTSANK	Ser^{114} (S2)
2[d]	3476.4	111–143 + P	LLYSPLIHTQSAVPVTI**pS**PNLVATATSTTSANK	Ser^{128} (S3)
3	3557.7	111–143 + 2P	**LLY**S**PLIHTQSAVPVTI**S**PNLVATATSTTSANK	ND[e]
4[d]	1088.8	147–157 + P	NKSNS**pS**PYLNK	Ser^{152} (S4)
4[d]	1088.8	147–157 + P	NKSN**pS**SPYLNK	Ser^{151}
5	936.5	202–209 + P	RV**pS**PVTAK	Ser^{204} (S5)
6[d]	2615.6	210–235 + P	TSSSAEGVVVASE**pS**PVIAPHGSSHSR	Ser^{223} (S6)
6[d]	2615.6	210–235 + P	TSSSAEGVVVA**S**E**S**PVIAPHGSSHSR	ND
7	2694.9	210–235 + 2P	**TSSSAEGVVVA**S**E**S**PVIAPHGSSHSR	ND
8[d]	1824.7	4–19 + P	T**T**SEGIHGFVDDLEPK	Thr^{4}/Thr^{5}[f]
8[d]	1824.7	4–19 + P	TT**pS**EGIHGFVDDLEPK	Ser^{6}
9	2659.5	160–184 + P	GKPGPDpSATSLFELPDSVIPTPKPK	Ser^{167}
10	1242.3	242–252 + P	S**S**GALVDDDKR	Ser^{242}/Ser^{243}[f]
11	1398.1	241–252 + P	RS**pS**GALVDDDKR	Ser^{243}
12	1554.2	240–252 + P	RRSpSGALVDDDKR	Ser^{242}
13	1634.2	240–252 + 2P	**RR**pSpS**GALVDDDKR	Ser^{242}, Ser^{243}
14	1526.1	*240–252 + P	*RRS**pS**GALVDDDKR	Ser^{243}
15	5069.6	37–79 + P	**HDGREDFNEQNDELNSQENHNSSENGNENENEQDSLALDDLDR	ND
16	5148.4	37–79 + 2P	**HDGREDFNEQNDELNSQENHNSSENGNENENEQDSLALDDLDR	ND

[a] Determined molecular weight.
[b] Predicted tryptic peptide plus phosphate from Pho4 (P07270).
[c] All sequences have been verified by tandem mass spectrometry unless where otherwise noted (**). Confirmed phosphorylation sites are shown in bold face as **pS** (phosphoserine). In cases were the site of phosphorylation is ambiguous, the ambiguous residues are underlined, and the likely sites of phosphorylation are shown in bold face. *, the peptide contains an unknown modification in the first two residues that resulted in a mass shift of minus 28 Da. We did not routinely observe this species.
[d] During LC-MS analysis peaks 2, 4, and 8 eluted from reverse phase chromatography as two peaks, each containing a single site of phosphorylation.
[e] ND, sites not determined.
[f] We were unable to distinguish between these two sites.

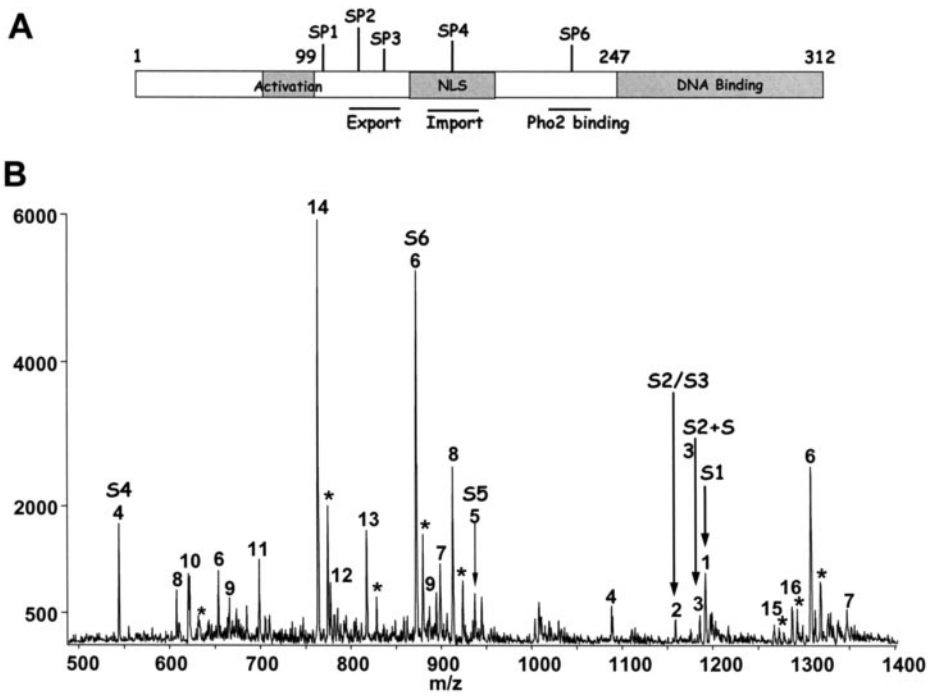

FIG. 2. **Phosphorylation profile of Pho4 grown in phosphate-rich medium.** *A*, linear schematic of Pho4 architecture showing previously identified Pho4 phosphorylation sites and their function. No function has been assigned to S1. All sites are substrates for the Pho80-Pho85 cyclin-Cdk complex. *B*, the precursor ion scan mass spectrum of trypsin-digested Pho4 shows more than 16 unique phosphopeptides. Peptides numbered *1–16* can be assigned to Pho4 sequences as listed in Table I. Peaks with the same number represent different charge states of the same peptide. Peaks marked with an asterisk (*) are sodium ion adducts of the preceding numbered peak.

(see Table I and Fig. 2*A*). The Pho80-Pho85 kinase has been shown to phosphorylate Pho4 *in vitro* on five of these sites S1, S2, S3, S4, and S6 (27). Two-dimensional phosphopeptide mapping demonstrated that peptides containing these *in vitro* sites co-migrated with a subset of ^{32}P metabolically labeled phosphopeptides contained in Pho4 from phosphate-rich medium and that these sites were absent in a *pho80* deletion strain (33). Four of these five sites have been given distinct roles in regulating Pho4 function (9). However, other than the specific analysis of these Cdk sites, little is known about the overall phosphorylation status of Pho4. Direct analysis of Pho4 phosphorylation is complicated by the extremely low expression of Pho4 in wild type yeast (34) with a reported codon bias index of −0.05 (35).

To establish the overall state of Pho4 phosphorylation we purified Pho4 as a GST-Pho4 fusion protein from yeast grown in phosphate-rich medium. Following SDS-PAGE and digestion with trypsin we examined the unfractionated digest using a precursor ion scan for *m/z* 79. The overall phosphorylation profile of Pho4 from phosphate-rich medium shows the presence of more than 16 different phosphopeptides (Fig. 2*B*). After matching the molecular weights of the tryptic phosphopeptides to the Pho4 sequence (P07270) we were able to identify sequences that contained at least 13 different sites. We found that peptides containing all six Cdk sites were phosphorylated *in vivo*, including the S1 site (Fig. 2*A*, *peak 1*), which was reported previously to be a poor *in vitro* substrate for Pho80-Pho85 (8) and was not detectable by two-dimensional phosphopeptide mapping (27). We also found phosphorylation on a peptide containing the S5 site (Fig. 2*A*, *peak 5*), which was reported previously not to be dependent on Pho80-Pho85 (27). To test whether phosphorylation of S5 is independent of Pho80-Pho85 we isolated Pho4 from a Pho85 deletion strain grown in normal medium. We found that phosphorylation of the S5 peptide was similar to that of Pho4 from the wild type Pho4 strain (data not shown). To verify that these peptides are indeed phosphorylated on the S1 and S5 sites we sequenced both peptides by tandem mass spectrometry. The data from these experiments identified phosphorylation on S1 and S5 exclusively. It is possible that both of these sites are utilized *in vivo* by a kinase other than Pho80-Pho85. The S2 and S3 sites are contained within a single tryptic peptide, and we found this peptide to be both singly and doubly phosphorylated (Fig. 2*A*, *peaks 2* and *3*, respectively). We also found the peptide containing S6 to be both singly and doubly phosphorylated (Fig. 2*A*, *peaks 6* and *7*, respectively). In addition to the seven peptides containing the Cdk consensus sites, 10 remaining peptides contained apparently novel sites (see Table I). One of these was contained in five different partial tryptic peptides (*peaks 10–14*) due to multiple lysine and arginine residues at either end of the proposed sequence. The S1 peptide, which contains four methionines and one tryptophan, was also observed in multiple forms due to extensive oxidation.

When yeast is deprived of phosphate, the Pho80-Pho85 complex is inactivated. Non-phosphorylated Pho4 then accumulates in the nucleus and activates expression of phosphate-responsive genes (27). Measuring changes in phosphorylation on low abundance proteins normally is accomplished using ^{32}P metabolic labeling. In the case of Pho4, however, this highly sensitive technique cannot be used because phosphate starvation is necessary to trigger the inhibitory response.

To test whether the NIT-precursor ion scan method could detect the phosphate responsiveness of the Pho4 phosphorylation sites, we grew yeast in phosphate-depleted and phosphate-rich medium and labeled the Pho4 derived from each with a d_0 or d_5 tag, respectively. After combining the samples we measured the relative change in stoichiometry at each site with a single precursor ion scan experiment. To correct the observed d_5/d_0 ratios for differences in the amount of starting protein we applied a normalization factor of 1.2 ± 0.1, which we determined by analyzing a small aliquot of the pooled sample by LC-MS and measuring the d_5/d_0 ratio for 10 non-phosphorylated Pho4 peptides. By way of comparison, we took a separate sample of yeast grown in phosphate-rich medium and split it in two, labeled the two halves with either d_0 or d_5 tag, recombined the halves, and analyzed it in the same way. Examples of the raw data from these two experiments are shown in Fig. 3, *A* and *B*. If phosphorylation at a given site is unaffected by a change in phosphate availability, the d_5/d_0 ratio should be close to 1.0. Phosphorylation sites that decrease in response to phosphate depletion will have a d_5/d_0 ratio greater than 1.0, and those that increase will have a ratio less than 1.0. The normalized d_5/d_0 ratio for each phosphopeptide from the phosphate-depleted/phosphate-rich analysis is listed in Fig. 3*C*. For larger peptides such as 1, 2, 3, and 9 (which are observed at charge states 3− and higher), although we can still detect changes greater than 2-fold, the limited mass resolution of the precursor ion scan does not allow us to accurately quantitate changes beyond 2-fold (for example see Supplemental Fig. S1). Therefore, the observed decrease for these peptides is reported as ≥2.0 In addition to the five previously described phosphate-dependent Cdk sites, many of the other peptides showed a change in phosphorylation stoichiometry in response to phosphate starvation.

The phosphorylation profile of Pho4 from normal medium shows that all six Cdk phosphorylation sites are utilized *in vivo* (Fig. 2*B*). However, the isotope labeling data comparing the phosphate-depleted and phosphate-rich Pho4 suggest that only S1, S2, S3, S4, and S6 are responsive to phosphate. The d_5/d_0 ratios for these five sites (Fig. 3*C*) all show a decrease in phosphorylation in the absence of phosphate in the growth medium. These data are consistent with the *in vivo* and *in vitro* biochemical data that show S1–S4 and S6 are substrates for Pho80-Pho85 and that the activity of Pho80-Pho85 Cdk complex is phosphate-dependent. Phosphorylation at S2, S3, S4, and S6 regulate Pho4 nuclear localization and transcriptional

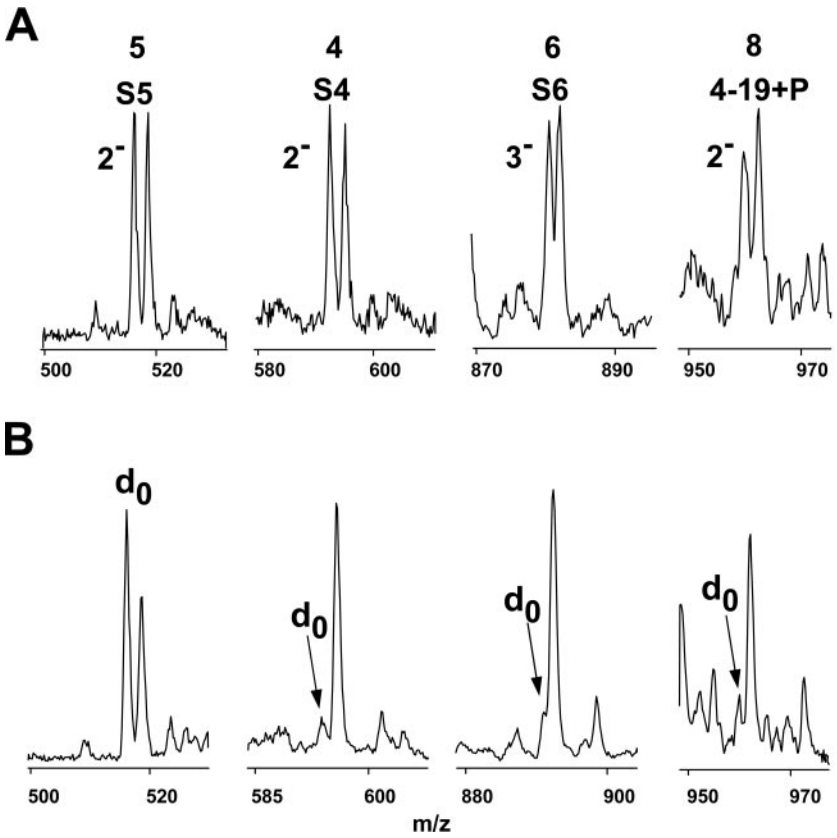

C

Peak	Peptide	Cdk Site	Change (d5/d0)
1	80-110 + P	S1	≥ 2.0
2	111-143 + P	S2/S3	≥ 2.0
3	111-143 + 2P	S2,S3	≥ 2.0
4	147-157 + P	S4	5.3
5	202-209 + P	S5	0.7
6	210-235 + P	S6	5.2
7	210-235 + 2P	S6	5.0
8	4-19 + P		3.0
9	160-184 + P		≥ 2.0
10	242-252 + P		1.5
11	241-252 + P		1.9
12	240-252 + P		ND
13	240-252 + 2P		1.5
14	*240-252 + P		1.5
15	37-79 + P		1.0
16	37-79 + 2P		1.0

FIG. 3. **Pho4 phosphorylation responds to changes in the availability of phosphate in the medium.** *A*, control sample showing d_5/d_0 ratios for select Pho4 peptides. Narrow *m/z* ranges from a single full mass range precursor ion scan are shown. Pho4 was grown in phosphate-rich medium, purified, and split into two samples. After labeling with d_0 or d_5 tags, the samples were recombined and analyzed using the NIT-precursor ion scan strategy. All pairs show a ratio close to 1.0 as expected. *B*, comparison of Pho4 from phosphate-depleted (d_0) and phosphate-rich (d_5) medium. After labeling, the samples were combined and analyzed using the NIT-precursor ion scan strategy. Narrow *m/z* ranges from a single full mass range precursor ion scan show the same peptides as seen in *A*. As predicted (9) phosphorylation sites such as S4 and S6, which are substrates for the Pho80-Pho85 kinase, decrease in abundance in the phosphate-depleted (d_0) media. Other sites such as S5 and the sequence 4–19 show unexpected changes when the cells are starved of phosphate. *C*, change in phosphorylation for all Pho4 phosphopeptides as measured by the NIT-precursor ion scan experiment. Using the ratio d_5/d_0, numbers greater than 1.0 indicate a decrease in phosphorylation in phosphate-depleted media. The d_5/d_0 ratio for peaks 2, 4, and 8 represent the combined change for the two monophosphorylated forms of each sequence. Due to the limited mass resolution of the experiment we were only able to accurately quantify changes up 2-fold for large peptides such as 1, 2, 3, and 9. The observed decrease for these peptides is reported as ≥2.0 *ND*, not determined.

activity (9); however, phosphorylation at S1 is reported to have no apparent role in Pho4 regulation (9). Because of the size of the S1 peptide and the fact that it undergoes differential oxidation at all four methionines, analysis of this peptide is very difficult. The absence of any observable d_0 form suggests a significant decrease in S1 phosphorylation in phosphate-depleted medium. Phosphorylation at S5, as expected, did not decrease under conditions of low phosphate. In fact this site showed a modest yet consistent increase in phosphorylation when yeast was grown in phosphate-depleted medium (Fig. 3, *A* and *B*). In this case, phosphorylation at S5 serves as an internal control showing that the decrease in phosphorylation observed at other sites is not merely the result of a breakdown in the phosphate transport system. In addition to the five Cdk sites, the d_5/d_0 ratios for a number of other peptides indicated that at least three novel phosphorylation sites contained in the sequences 4–19, 241–252, and 160–184 were also affected by phosphate availability (Fig. 3*C*).

To confirm the Cdk sites and conclusively identify the novel sites of phosphorylation that responded to phosphate availability, we sequenced peptides for each unique phosphorylation site by tandem mass spectrometry (The annotated mass spectrum (40) for each uniquely identified phosphorylation site can be found in Supplemental Fig. S2A–J). We found that the monophosphorylated S2/S3 peptide chromatographed as two species, one containing phosphorylation at Ser^{114} (S2) and the other containing phosphorylation at Ser^{128} (S3). The presence of the S2/S3 peptide in three forms (two singly and one doubly phosphorylated) is consistent with the published two-dimensional ^{32}P-phosphopeptide mapping data for Pho4 from phosphate-rich medium that showed that peptides con-

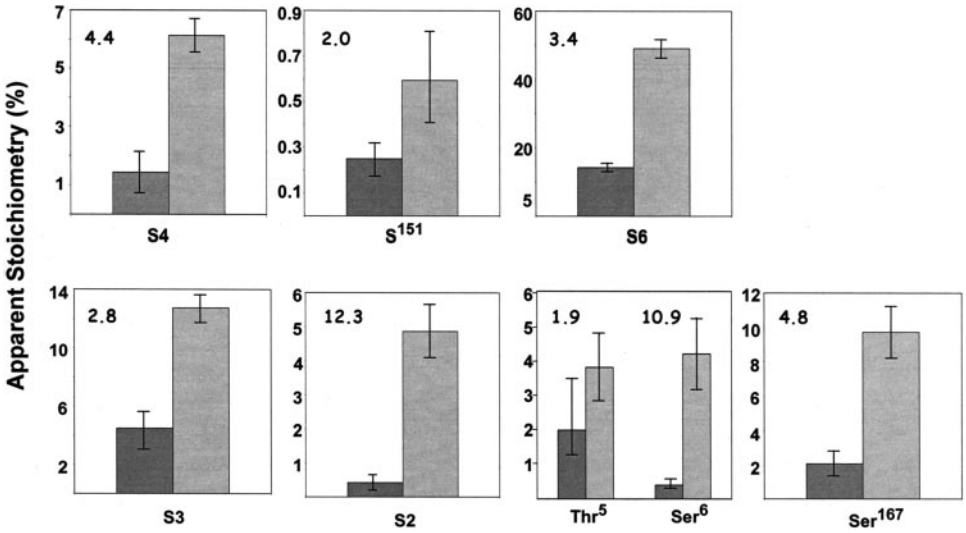

FIG. 4. **Phosphate-responsive change in select Pho4 phosphorylation sites as measured by LC-SRM.** Pho4 from either three normal (*light*) or two phosphate-depleted (*dark*) cultures was processed and analyzed as described under "Experimental Procedures." The -fold change in average apparent stoichiometry between normal and phosphate-depleted media is shown as an *inset*.

taining these sites migrated as multiple spots. While confirming phosphorylation at S4 (Ser^{152}), we found that the peptide containing S4 also chromatographed as two distinct phosphopeptides. We identified the second site as Ser^{151}. Two-dimensional ^{32}P-phosphopeptide mapping data showed that the *in vivo* ^{32}P-labeled S4 peptide also mapped as two spots with one of the spots being retained in a *pho80* knockout strain (33). While confirming phosphorylation at S6, we also identified a very small amount of a second monophosphorylated peptide; however, we were unable to determine the site of labeling. As mentioned previously we also confirmed that the S1 (Ser^{100}) and S5 (Ser^{204}) sites were phosphorylated. The identification of all the unique sites is presented in Table I. In addition to the six Cdk sites, we conclusively identified six additional, novel phosphorylation sites at Thr^5, Ser^6, Ser^{151}, Ser^{167}, Ser^{242}, and Ser^{243} (see Table I). The peptide 4–19 + P eluted as two monophosphorylated peptides. On the later eluting peptide we were able to assign phosphorylation to Ser^6. In the case of the early eluting peptide, we were unable to distinguish between phosphorylation at any of the first three residues. Because it is less likely that trypsin would efficiently cleave between Arg^3 and Thr^4, we conclude that this sequence is most likely phosphorylated at Thr^5. Phosphorylation at Ser^{243} was found in several peptides due to the presence of multiple lysine and arginine residues at either end of the sequence surrounding it.

To obtain a more accurate representation of the change in Pho4 phosphorylation at the phosphate-responsive sites we used LC-MS with selected reaction monitoring (SRM). Using the MS/MS spectra as a guide we chose an abundant, high mass fragment ion for each phosphate-responsive peptide and using a triple quadrupole mass spectrometer created a set of SRM functions to measure the specific fragment ion production of each peptide precursor (see Supplemental Table S1). By continuously cycling between the SRMs during an LC-MS analysis, we measured the abundance of each phosphopeptide in the Pho4 sample. In the same set of LC-MS analyses, we also monitored for the production of the same fragment ion from the non-phosphorylated counterpart of each phosphopeptide of interest. Using the measured abundance of each phosphorylated form of a given sequence and the measured abundance of the non-phosphorylated form we calculated an apparent stoichiometry for each phosphorylation site. Although this stoichiometry may not be accurate due to a difference in the ionization efficiencies for the phosphorylated and non-phosphorylated peptides in each set, experience in our laboratory and others suggests that this measure is frequently a reasonable approximation (25, 36, 37). Furthermore because the ionization efficiencies for peptides in any given experimental system will be constant, we can use the value for the apparent stoichiometry to measure relative changes in site-specific phosphorylation. Using this strategy it is not necessary to normalize the peptide abundance measurements for protein load. An alternative to using the non-phosphorylated analog to derive relative quantitation would be to use several other non-phosphorylated peptides from each sample to normalize the abundance measurements (38). If a more accurate measure of absolute stoichiometry is required, the ionization efficiency of each peptide would have to be determined empirically (17, 38).

We first used the LC-SRM method to understand the experimentally introduced variation in our measurements. A single Pho4 culture grown in normal media was divided into four aliquots and processed as described. We then measured the extent of phosphorylation at each of the phosphate-responsive sites. From these data we determined that the analytical

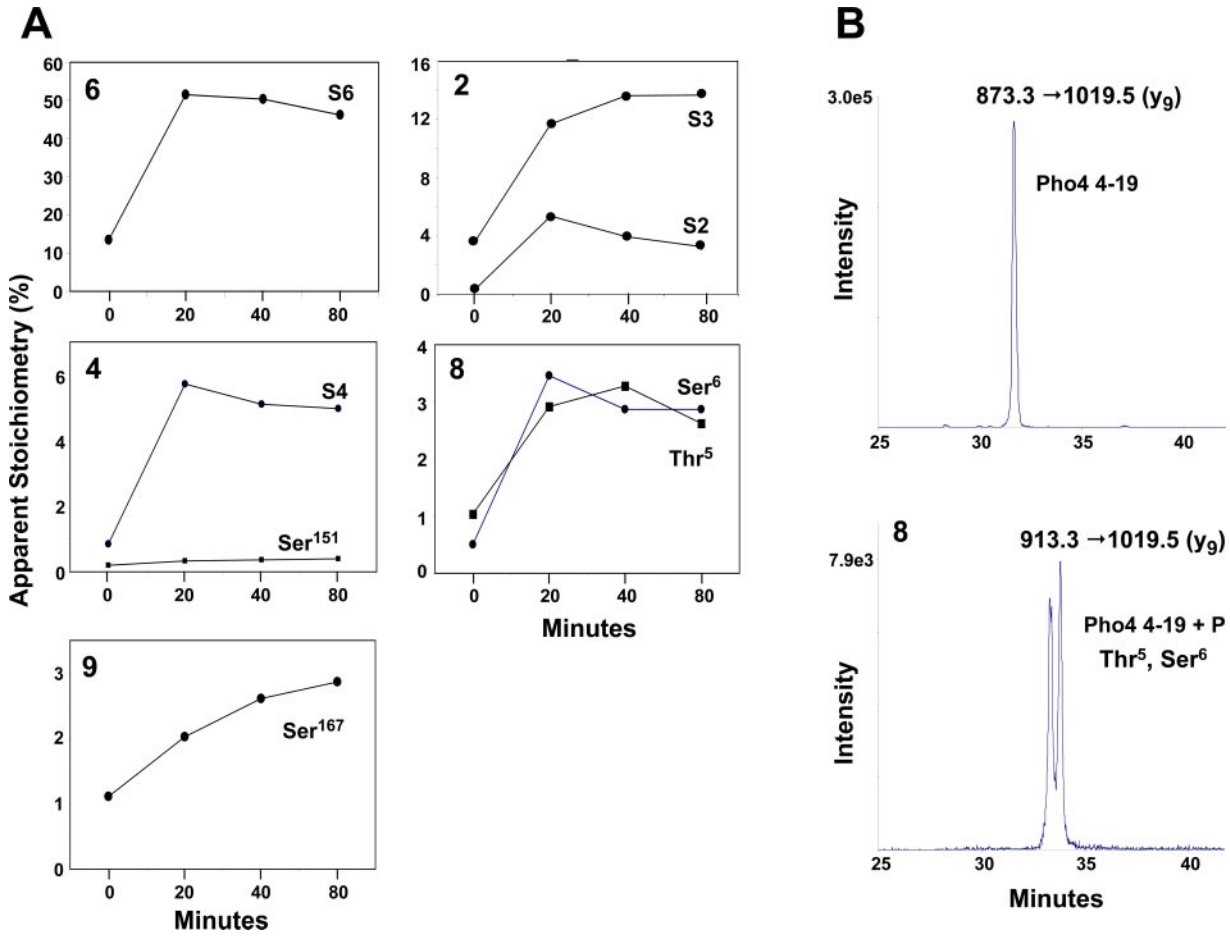

FIG. 5. **Time course analysis of phosphate-responsive Pho4 phosphorylation.** Pho4 expression was induced in yeast growing in phosphate-free medium. After treatment with cycloheximide to halt further protein synthesis, yeast cells were transferred into phosphate-rich medium, and cells were sampled at the indicated time points to measure Pho4 phosphorylation. *A*, phosphorylation stoichiometry for individual phosphate-responsive Pho4 peptides. The abundance of each phosphorylated and corresponding non-phosphorylated Pho4 sequence was monitored by LC-SRM. Peptides 2, 4, and 8 were monophosphorylated on two different sites. In each case the two phosphoforms could be separated chromatographically. *B*, LC-SRM chromatogram for the non-phosphorylated (*top*) and phosphorylated (*bottom*) Pho4 peptide 4–19 80 min after phosphate-starved yeast were shifted into phosphate-rich medium. The sequence is monophosphorylated on two distinct sites (*bottom*). The SRM transition for each species uses an *m/z* 1019.5 fragment ion (y_9) that is common to all three peptides. The distance of the y_9 cleavage from Thr^5 and Ser^6 minimizes the influence that the site of phosphorylation might have on the fragmentation efficiency.

variability in the entire protocol was 7% on average across all sites. We did not analyze phosphorylation at S1 or Ser^{243} due to the complex pattern of peptides produced from these two sequences.

We then grew replicate cultures in either normal or phosphate-depleted medium, and after purifying and trypsin-digesting Pho4 we measured the extent of phosphorylation at each of the eight sites by LC-SRM. A summary of the results for each of the eight peptides is presented in Fig. 4. An example of the data collected for the peptide 4–19 + P (*peak 8*) is shown in Fig. 5*B*. Compare the excellent signal to noise shown in these data with the full scan data shown in Figs. 2*B* and 3*B*. Approximately 50-fold less Pho4 was used in the SRM analyses. The high sensitivity and dynamic range of the LC-SRM experiments allowed us to derive reliable measurements even when the apparent stoichiometry is between 1 and 5%. Using the LC-SRM method we were able to derive more accurate -fold change data for the large peptides (which proved difficult for the NIT-precursor scan method), S2, S3, and Ser^{167}, and because of the chromatographic resolution of the LC-MS system we were able to obtain separate values for the each of the monophosphorylated positional isomers. The -fold change for each of the eight phosphorylation sites is shown in Fig. 4, *insets*.

To better understand the complex nature of the Pho4 phosphate-dependent phosphorylation profile, we analyzed the change in stoichiometry at the functionally relevant sites as Pho4 adapts to a change in the phosphate environment. We induced expression of Pho4 in yeast growing in phosphate-depleted medium. Under these conditions ($t = 0$) the phosphate-responsive sites should be largely unphosphorylated. We then treated the cells with cycloheximide to stop further

protein synthesis. Phosphorylation of Pho4 was triggered by the addition of phosphate to the culture. Equal aliquots of culture were sampled at 0, 20, 40, and 80 min. We then measured the extent of phosphorylation at each of the phosphate-responsive sites over time. The phosphorylation time course for each of the eight sites is shown in Fig. 5*A*.

Direct fluorescence microscopy shows that green fluorescent protein-labeled Pho4 is exported from the nucleus within 6 min of yeast being shifted into phosphate-rich medium (29). Consistent with this, our data show that most of the phosphate-responsive sites have reached their maximum level of phosphorylation at or before the 20-min time point (Fig. 5*A*). Although not substrates for Pho80-Pho85, the response curves for Thr^5 and Ser^6 also reach their maxima by 20 min and have the same profile as the Cdk sites S2, S4, and S6. The two sites that did not reach an early maximum, S3 and Ser^{167}, both showed more gradual increases in phosphorylation. Ser^{151}, found on the same peptide that contains the Cdk site S4, was unresponsive to phosphate.

Regardless of the shape of the phosphate-response curve, we found that the maximum level of phosphorylation differed among all sites and in particular the Cdk sites. Under physiological levels of expression, most if not all of Pho4 appears to be phosphorylated in phosphate-rich medium (9), although no direct site-specific measurements have been reported. In our experiments, the substoichiometric phosphorylation of Pho4 in phosphate-rich medium may result from the high level of overexpression relative to endogenous Pho4 and a limiting amount of the Pho80-Pho85 kinase. If this is the case the difference in stoichiometry at the various sites may reflect the distinct site preferences that Pho80-Pho85 shows for Pho4 *in vitro* (39). In our experiments the S6 site, which regulates the binding of Pho4 to the transcription factor Pho2 and the *PHO5* promoter, is phosphorylated to the greatest extent insuring that transcription of phosphate-responsive genes is halted as soon as possible. Phosphorylation of S2 and S3 is required for export of Pho4 from the nucleus. Interestingly these two sites are phosphorylated to different extents and have differently shaped phosphate-response curves. The apparent stoichiometry at S4 is comparable with the level of phosphorylation at S2. Because phosphorylation at S4 blocks nuclear import of Pho4 and phosphorylation at S2 and S3 is required for export, the equivalent stoichiometry at these sites ensures that any Pho4 exported from the nucleus is not immediately reimported. Taken together, these *in vivo* data support the notion that Pho4 is phosphorylated at each critical site before it is exported from the nucleus (39). These *in vivo* results are in perfect agreement with published *in vitro* data (39) showing that phosphorylation of Pho4 is semiprocessive with S6, S2/S3, and S4 being phosphorylated on the same molecule but with a marked preference in the order S6 (60%) $>$ S2/S3 (24%) $>$ S4 (16%).

The apparent stoichiometry at Ser^{167}, Thr^5, and Ser^6 is low but comparable with the levels measured in these experiments for S2, S4, and S1 (S1 data not shown). Phosphorylation at Ser^{243} (estimated from separate experiments) appears to be greater than for any other phosphate-responsive site with the possible exception of S6. We estimate the stoichiometry at Ser^{243} to be on the order of 30–50%. Although the functional significance of phosphorylation of Ser^{243}, Ser^{167}, Thr^5, and Ser^6 is not known, these sites clearly show phosphate responsiveness, and the time-dependent phosphorylation profile of the latter three mimics the Cdk-responsive sites. Further study will be required to determine whether these sites can be assigned a role in Pho4 regulation.

Conclusions—We have presented a results-driven, quantitative strategy for determining the functional significance of site-specific protein phosphorylation. The strategy is based on stable isotope labeling of each and every peptide in a protein sample and analysis by mass spectrometry using a phosphopeptide-selective precursor ion scan. It requires no prior knowledge of the phosphorylation profile of a protein. For simple mixtures, such as those derived by protein immunoprecipitation, no prefractionation or phosphopeptide enrichment is necessary. For samples from two different conditions, changes in phosphorylation at all detectable epitopes can be quantitated in a single experiment. Using these data as a guide, only those phosphorylation sites showing a functionally significant change need be identified and studied in greater detail. More accurate quantitation or detailed kinetic characterization of these sites can then be conducted without isotope labeling.

In this work we used a chemical labeling strategy to incorporate the isotopic tag used for quantitation (15). We chose the described approach because it labels each peptide in a sample only once at the N terminus. The reactions are simple to carry out, and the reagents are inexpensive and available from any number of commercial suppliers. Metabolic labeling techniques such as SILAC (stable isotope labeling by amino acids in cell culture) (11) or any other chemical labeling strategies would be equally suitable for the described strategy as long there is the potential to label every peptide. To detect and quantitate every phosphorylation site in a sample, it is important that each and every peptide be labeled.

The use of the mass spectrometry-based precursor ion scan for phosphate provides an unbiased analysis of the phosphorylation profile of a sample. This technique readily detects substoichiometric phosphorylation at levels below 1%. Because it selectively detects only the phosphorylated peptides in a sample, it is not necessary for the sample to be purified or enriched prior to analysis. In this work we analyzed multiple phosphorylation sites in unfractionated protein digests. More complex samples such as multiprotein complexes would require fractionation at either the protein or peptide level. Recently we have begun to explore the possibility of using on-line LC-MS coupled with fast precursor ion

scanning to analyze more complex samples.[2]

A limitation of the precursor scan is the low mass resolution of the experiment. The 5-dalton mass difference of the isotopically labeled pairs was readily resolved on doubly charged ions up to approximately *m/z* 1400; however, at *m/z* 1000 the separation of the differentially labeled pair was only ~50% (see peptide 4–19 + P in Fig. 3*A* and Supplemental Fig. S1). Thus for doubly and triply charged ions, although we can detect changes greater than 2-fold, we cannot accurately quantitate this change for *m/z* values above 1400 and *m/z* 1100, respectively (an example of the latter is shown in Supplemental Fig. S1). We are exploring the possibility of a tag with a greater mass shift. To facilitate applications that benefit from up-front chromatography, we are also investigating a tag that uses carbon and nitrogen isotopes in place of deuterium. Although the low mass resolution of the precursor scan somewhat limits the accuracy of the quantitation, it is more than sufficient to identify those peptides that show a functionally significant increase or decrease in phosphorylation.

As part of the results-driven strategy, we used the precursor ion scan data to select peptides for further study by more sensitive, targeted MS techniques. Using LC-SRM we are able to obtain more accurate quantitative data on the precursor ion-selected epitopes in a straight forward manner without the use of isotopes. Because the mass spectrometer is not scanning a wide mass range but rather detecting only those few ions related to the peptides of interest, the LC-SRM method greatly improved the sensitivity and dynamic range of the quantitation. In the case of Pho4, using chromatographic separation and 10 SRM functions we were able to derive quantitative data on eight phosphorylation sites in a single analysis with ~50-fold less material than in the isotope labeling experiment. Modern triple quadrupole mass spectrometers are able to easily monitor 25 or more SRM functions in a single cycle. By grouping SRM functions into discreet time bins, it is possible to monitor several hundred transitions with high sensitivity over the elution profile of a sample. This raises the possibility that this type of two-layer approach to phosphorylation site quantitation could be done on a proteome scale if proper fractionation is used. The recent introduction of a hybrid triple quadrupole-linear ion trap mass spectrometer now allows all aspects of the described experiments to be done on a single instrument with the highest levels of sensitivity available.

We studied the phosphate-responsive phosphorylation of Pho4 to show that the methods described here could identify functionally relevant phosphorylation sites on proteins. Much is known about the manner in which phosphorylation of select consensus Cdk sites regulates the transcriptional activity of Pho4 in response to changes in phosphate availability (8, 27–29). Our results show that phosphorylation at five of the six potential Cdk sites increases when yeast are shifted from a phosphate-depleted to a phosphate-rich medium. This is consistent with earlier published studies that used site-specific phosphomutants to define the role of the five Cdk sites in regulating Pho4 function (9). The work presented here represents the first direct, quantitative, *in vivo* biochemical evidence for the phosphate-responsive phosphorylation of these five Cdk sites. As measured here, the differences in apparent stoichiometry at the five sites can be rationalized in terms of the selectivity of the Pho80-Pho85 kinase and the requirement to efficiently shut off transcription of Pho4-responsive genes. Because our methodology requires no prior knowledge of the phosphorylation profile of a protein and is unbiased in its detection selectivity, we were able to identify and quantitate four novel phosphorylation sites (Ser^{243}, Ser^{167}, Thr^{5}, and Ser^{6}) that also responded to phosphate availability. What role, if any, these new sites have in regulating Pho4 function remains to be determined. Although we and others have shown that the Cdk site S1 is phosphorylated in response to phosphate availability, no role for this site has yet been identified.

Acknowledgments—We are grateful to Caretha Creasy, Megan McLaughlin, and Yun Liu from the GlaxoSmithKline Pathway Genomics group for providing the GST-PHO4 yeast strain and for technical advice on various aspects of yeast cell culture. We are also indebted to Prof. Raymond Deshaies, Division of Biology at California Institute of Technology, for advice on preparing the Pho4 time point experiments and Prof. Erin O'Shea, Department of Cell Biology at Harvard, for helpful discussion of this work. Finally we thank our co-workers Susan Loughrey Chen and Dean McNulty for careful reading of the manuscript.

* The costs of publication of this article were defrayed in part by the payment of page charges. This article must therefore be hereby marked "*advertisement*" in accordance with 18 U.S.C. Section 1734 solely to indicate this fact.

S The on-line version of this article (available at http://www.mcponline.org) contains supplemental material.

‡ To whom correspondence should be addressed. E-mail: Roland_S_Annan@gsk.com.

[2] M. J. Huddleston and R. S. Annan, unpublished data.

REFERENCES

1. Karcher, R. L., Roland, J. T., Zappacosta, F., Huddleston, M. J., Annan, R. S., Carr, S. A., and Gelfand, V. I. (2001) Cell cycle regulation of myosin-V by calcium/calmodulin-dependent protein kinase II. *Science* **293,** 1317–1320
2. Verma, R., Annan, R. S., Huddleston, M. J., Carr, S. A., Reynard, G. and Deshaies, R. J. (1997) Phosphorylation of Sic1p by G1 Cdk required for its degradation and entry into S phase. *Science* **278,** 455–560
3. Pawson, T. (2004) Specificity in signal transduction: from phosphotyrosine-SH2 domain interactions to complex cellular systems. *Cell* **116,** 191–203
4. Geymonat, M., Spanos, A., Wells, G. P., Smerdon, S. J., and Sedgwick, S. G. (2004) Clb6/Cdc28 and Cdc14 regulate phosphorylation status and cellular localization of Swi6. *Mol. Cell Biol.* **6,** 2277–2285
5. Blume-Jensen, P., and Hunter, T. (2001) Oncogenic kinase signalling. *Nature* **411,** 355–365
6. Manning, G. Whyte, D. B., Martinez, R., Hunter, T., and Sudarsanam, S. (2002) The protein kinase complement of the human genome. *Science* **298,** 1012–1912-1934
7. Cohen, P. (2000) The regulation of protein function by multisite phosphorylation—a 25 year update. *Trends Biochem. Sci.* **25,** 596–601
8. Nash, P., Tang, X., Orlicky, S., Chen, Q., Gertler, F. B., Mendenhall, M. D., Sicheri, F., Pawson, T., and Tyers, M. (2001) Multisite phosphorylation of

a CDK inhibitor sets a threshold for the onset of DNA replication. *Nature* **414,** 514–521
9. Komeili, A., and O'Shea, E. K. (1999) Roles of phosphorylation sites in regulating activity of the transcription factor Pho4. *Science* **284,** 977–980
10. Gygi, S. P., Rist, B., Gerber, S. A., Turecek, F., Gelb, M. H., and Aebersold, R. (1999) Quantitative analysis of complex protein mixtures using isotope-coded affinity tags. *Nat. Biotechnol.* **17,** 994–999
11. Ong, S. E., Blagoev, B., Kratchmarova, I., Kristensen, D. B., Steen, H., Pandey, A., and Mann, M. (2002) Stable isotope labeling by amino acids in cell culture, SILAC, as a simple and accurate approach to expression proteomics. *Mol. Cell. Proteomics* **1,** 376–386
12. Hunter, T. C., Yang, L., Zhu, H., Majidi, V., Bradbury, E. M., and Chen, X. (2001) Peptide mass mapping constrained with stable isotope-tagged peptides for identification of protein mixtures. *Anal. Chem.* **73,** 4891–4902
13. Oda, Y., Huang, K., Cross, F. R., Cowburn, D., and Chait, B. T. (1999) Accurate quantitation of protein expression and site-specific phosphorylation. *Proc. Natl. Acad. Sci. U. S. A.* **96,** 6591–6596
14. Veenstra, T. D., Martinovic, S., Anderson, G. A., Pasa-Tolic, L., and Smith, R. D. (2000) Proteome analysis using selective incorporation of isotopically labeled amino acids. *J. Am. Soc. Mass Spectrom.* **11,** 78–82
15. Zappacosta, F., and Annan, R. S. (2004) N-terminal isotope tagging strategy for quantitative proteomics: results-driven analysis of protein abundance changes. *Anal. Chem.* **76,** 6618–6627
16. Bonenfant, D., Schmelzle, T., Jacinto, E., Crespo, J. L., Mini, T., Hall, M. N., and Jenoe, P. (2003) Quantitation of changes in protein phosphorylation: a simple method based on stable isotope labeling and mass spectrometry. *Proc. Natl. Acad. Sci. U. S. A.* **100,** 880–885
17. Gerber, S. A., Rush, J., Stemman, O., Kirschner, M. W., and Gygi, S. P. (2003) Absolute quantification of proteins and phosphoproteins from cell lysates by tandem MS. *Proc. Natl. Acad. Sci. U. S. A.* **100,** 6940–6945
18. Gruhler, A., Olsen, J. V., Mohammed, S., Mortensen, P., Faergeman, N. J., Mann, M., and Jensen, O. N. (2005) Quantitative phosphoproteomics applied to the yeast pheromone signaling pathway. *Mol. Cell. Proteomics* **4,** 310–327
19. Ibarrola, N., Molina, H., Iwahori, A., and Pandey, A. (2004) A novel proteomic approach for specific identification of tyrosine kinase substrates using [^{13}C]tyrosine. *J. Biol. Chem.* **279,** 15805–15813
20. Salomon, A. R., Ficarro, S. B., Brill, L. M., Brinker, A., Phung, Q. T., Ericson, C., Sauer, K., Brock, A., Horn, D. M., Schultz, P. G., and Peters, E. C. (2003) Profiling of tyrosine phosphorylation pathways in human cells using mass spectrometry. *Proc. Natl. Acad. Sci. U. S. A.* **100,** 443–448
21. Posewitz, M. C., and Tempst, P. (1999) Immobilized gallium(III) affinity chromatography of phosphopeptides. *Anal. Chem.* **71,** 2883–2892
22. Rush, J., Moritz, A., Lee, K. A., Guo, A., Goss, V. L., Spek, E. J., Zhang, H., Zha, X. M., Polakiewicz, R. D., and Comb, M. J. (2005) Immunoaffinity profiling of tyrosine phosphorylation in cancer cells. *Nat. Biotechnol.* **23,** 94–101
23. Griffin, T. J., Lock, C. M., Li, X. J., Patel, A., Chervetsova, I., Lee, H., Wright, M. E., Ranish, J. A., Chen, S. S., and Aebersold, R. (2003) Abundance ratio-dependent proteomic analysis by mass spectrometry. *Anal. Chem.* **75,** 867–874
24. Graber, A., Juhasz, P. S., Khainovski, N., Parker, K. C., Patterson, D. H., and Martin, S. A. (2004) Result-driven strategies for protein identification and quantitation—a way to optimize experimental design and derive reliable results. *Proteomics* **4,** 474–489
25. Carr, S. A., Huddleston, M. J., and Annan, R. S. (1996) Selective detection and sequencing of phosphopeptides at the femtomole level by mass spectrometry. *Anal. Biochem.* **239,** 180–192
26. Wilm, M. Neubauer, G., and Mann, M. (1996) Parent ion scans of unseparated peptide mixtures. *Anal. Chem.* **68,** 1–27
27. O'Neill, E. M. Kaffman, A. Jolly, E. R., and O'Shea, E. K. (1994) Regulation of PHO4 nuclear localization by the PHO80-PHO85 cyclin-CDK complex. *Science* **271,** 209–212
28. Kaffman, A. Rank, N. M., and O'Shea, E. K. (1998) Phosphorylation regulates association of the transcription factor Pho4 with its import receptor Pse1/Kap121. *Genes Dev.* **12,** 2673–2683
29. Kaffman, A. Rank, N. M., O'Neill, E. M. Huang, L. S., and O'Shea, E. K. (1998) The receptor Msn5 exports the phosphorylated transcription factor Pho4 out of the nucleus. *Nature* **396,** 482–486
30. Joyal, J. L., Annan, R. S., Ho, Y. D., Huddleston, M. E., Carr, S. A., Hart, M. J., and Sacks, D. B. (1997) Calmodulin modulates the interaction between IQGAP1 and Cdc42. Identification of IQGAP1 by nanoelectrospray tandem mass spectrometry. *J. Biol. Chem.* **272,** 15419–15425
31. Zhang, X. Jin, Q. K. Carr, S. A., and Annan, R. S. (2002) N-terminal peptide labeling strategy for incorporation of isotopic tags: a method for the determination of site-specific absolute phosphorylation stoichiometry. *Rapid Commun. Mass Spectrom.* **16,** 2325–2332
32. Oshima, Y. (1997) The phosphatase system in Saccharomyces cerevisiae. *Genes Genet. Syst.* **72,** 323–334
33. Kaffman, A. Herskowitz, I., Tjian, R., and O'Shea, E. K. (1994) Phosphorylation of the transcription factor PHO4 by a cyclin-CDK complex, PHO80-PHO85. *Science* **263,** 1153–1156
34. Ghaemmaghami, S., Huh, W. K., Bower, K., Howson, R. W. Belle, A., Dephoure, N., O'Shea, E. K., and Weissman, J. S. (2003) Global analysis of protein expression in yeast. *Nature* **425,** 737–741
35. Garrels, J. I., Payne, W. E., and Hecht, R., Eds. (1997) *The Yeast Proteome Handbook*, 2nd Ed., p. 207, Proteome Inc., Beverly, MA
36. Guo, L., Kozlosky, C. J., Ericson, L. H., Daniel, T. O., Cerretti, D. P., and Johnson, R. S. (2003) Studies of ligand-induced site-specific phosphorylation of epidermal growth factor receptor. *J. Am. Soc. Mass Spectrom.* **14,** 1002–1031
37. Hegeman, A. D., Harms, A. C., Sussman, M. R., Bunner, A. E., and Harper, J. E. (2004) An isotope labeling strategy for quantifying the degree of phosphorylation at multiple sites in proteins. *J. Am. Soc. Mass Spectrom.* **15,** 647–653
38. Steen, H., Jebanathirajah, J. A., Springer, M., and Kirschner, M. W. (2005) Stable isotope-free relative and absolute quantitation of protein phosphorylation stoichiometry by MS. *Proc. Natl. Acad. Sci. U. S. A.* **102,** 3948–3953
39. Jeffery, D. A., Springer, M., King, D. S., and O'Shea, E. K. (2001) Multi-site phosphorylation of Pho4 by the cyclin-CDK Pho80-Pho85 is semi-processive with site preference. *J. Mol. Biol.* **306,** 997–1010
40. Biemann, K. (1990) Appendix 5. Nomenclature for peptide fragment ions (positive ions), in *Methods in Enzymology* (McCloskey, J. A., ed) Vol. 193, pp. 886–887, Academic Press, New York
41. Rubin, G. M. (1974) Three forms of the 5.8-S ribosomal RNA species in Saccharomyces cerevisiae. *Eur. J. Biochem*. **41,** 197–202